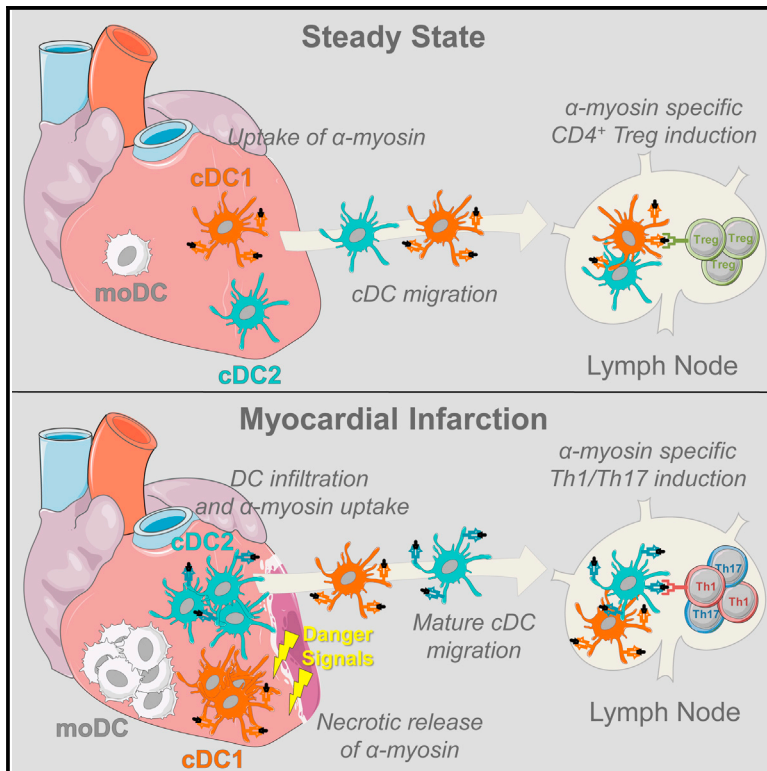


Myocardial Infarction Primes Autoreactive T Cells through Activation of Dendritic Cells

Graphical Abstract



Authors

Katrien Van der Borght, Charlotte L. Scott, Veronika Nindl, ..., Martin Guillems, Peter Carmeliet, Bart N. Lambrecht

Correspondence

peter.carmeliet@vib-kuleuven.be (P.C.), bart.lambrecht@ugent.be (B.N.L.)

In Brief

Van der Borght et al. demonstrate that myocardial infarction induces the priming of autoreactive CD4⁺ T cells specific for cardiac self-antigen α -myosin in the heart-draining lymph node through the maturation and migration of conventional dendritic cells. Using ex vivo co-culture systems, cDC2s are shown to be superior in presenting α -myosin.

Highlights

- IRF8⁺ cDC1, IRF4⁺ cDC2, moDCs, and macrophages are the APCs of the murine heart
- Self-antigen presentation in the steady state drives Treg development via cDC1s
- Myocardial infarction promotes infiltration, activation, and maturation of all DCs
- Myocardial infarction promotes priming of Th1/Th17 autoreactive T cells via cDC2s

Accession Numbers

GSE94949



Myocardial Infarction Primes Autoreactive T Cells through Activation of Dendritic Cells

Katrien Van der Borght,^{1,2} Charlotte L. Scott,^{1,4} Veronika Nindl,⁵ Ann Bouché,³ Liesbet Martens,^{1,2,4} Dorine Sichien,^{1,4} Justine Van Moorleghem,^{1,2} Manon Vanheerswyngheles,^{1,2} Sofie De Prijck,^{1,4} Yvan Saeys,^{1,2,4} Burkhard Ludwig,⁵ Thierry Gillebert,² Martin Guillailliams,^{1,4} Peter Carmeliet,^{3,*} and Bart N. Lambrecht^{1,2,6,7,*}

¹Immunoregulation and Mucosal Immunology, VIB Center for Inflammation Research, 9052 Ghent, Belgium

²Department of Internal Medicine, Ghent University, 9000 Ghent, Belgium

³VIB Vesalius Research Center, 3000 Leuven, Belgium

⁴Department of Biomedical Molecular Biology, Ghent University, 9000 Ghent, Belgium

⁵Institute of Immunobiology, Kantonsspital St. Gallen, 9007 St. Gallen, Switzerland

⁶Department of Pulmonary Medicine, ErasmusMC, 3015 Rotterdam, the Netherlands

⁷Lead Contact

*Correspondence: peter.carmeliet@vib-kuleuven.be (P.C.), bart.lambrecht@ugent.be (B.N.L.)

<http://dx.doi.org/10.1016/j.celrep.2017.02.079>

SUMMARY

Peripheral tolerance is crucial for avoiding activation of self-reactive T cells to tissue-restricted antigens. Sterile tissue injury can break peripheral tolerance, but it is unclear how autoreactive T cells get activated in response to self. An example of a sterile injury is myocardial infarction (MI). We hypothesized that tissue necrosis is an activator of dendritic cells (DCs), which control tolerance to self-antigens. DC subsets of a murine healthy heart consisted of IRF8-dependent conventional (c)DC1, IRF4-dependent cDC2, and monocyte-derived DCs. In steady state, cardiac self-antigen α -myosin was presented in the heart-draining mediastinal lymph node (mLN) by cDC1s, driving the proliferation of antigen-specific CD4⁺ TCR-M T cells and their differentiation into regulatory cells (Tregs). Following MI, all DC subsets infiltrated the heart, whereas only cDCs migrated to the mLN. Here, cDC2s induced TCR-M proliferation and differentiation into interleukin-(IL)-17/interferon-(IFN) γ -producing effector cells. Thus, cardiac-specific autoreactive T cells get activated by mature DCs following myocardial infarction.

INTRODUCTION

Autoreactive CD4⁺ T cells are normally deleted during thymic negative selection, yet many self-reactive T cells escape this checkpoint, emerging as anergic, thymic regulatory (tTreg) or ignorant conventional T cells (Tconv) (Davis, 2015). Self-reactive T cell activation is a major culprit in autoimmune disease, and therefore tolerance to some tissue-restricted self-antigens is shaped entirely by extrathymic processes. Suppression of autoreactive CD4⁺ T cells is dependent on peripheral dendritic cells (DCs), which present tissue-restricted self-antigens derived mostly from turnover of apoptotic cells (Steinman et al., 2003).

In the absence of inflammation, self-antigen presentation by DCs results in T cell anergy, further expansion of tTregs, or generation of induced (i)Tregs from Tconv cells, thus promoting peripheral tolerance to the self-antigen (Ganguly et al., 2013). Lack of steady-state DCs results in loss of functional Tregs and subsequent activation of autoreactive Th1/Th17 effector cells, whereas increased numbers of immature DCs result in increased iTreg numbers, which prevent autoimmunity (Ohnmacht et al., 2009; Darrasse-Jèze et al., 2009). It is, however, equally important that DCs presenting self-antigen remain in a quiescent state, devoid of cytokine production that can break peripheral tolerance (Eriksson et al., 2003; Ardouin et al., 2016). Removal of inhibitory nuclear factor (NF)- κ B signaling intermediates or artificial extension of DC life-span are sufficient to break self-tolerance (Kool et al., 2011; Stranges et al., 2007). Despite experiments clearly implicating DCs in the regulation of peripheral tolerance and induction of autoimmunity, the precise triggers that cause DC activation and possibly break self-tolerance are incompletely understood (Ganguly et al., 2013). Certain organ-directed infections trigger tissue-specific autoimmunity by promoting DC activation either through direct infection or release of cytokines that cause full DC maturation (Gangaplara et al., 2012; Torchinsky et al., 2009). Endogenous danger signals like uric acid or HMGB1 lead to DC maturation in response to sterile tissue injury (Scaffidi et al., 2002). Exposure of DCs to necrotic cells is sufficient to drive DC maturation in vitro (Gallucci et al., 1999). But currently, it is not known if sterile inflammation induced by tissue ischemia and necrosis causes DCs to drive the initiation of adaptive immune responses to self-antigen in vivo.

To address this, we chose a model of myocardial infarction (MI). Undoubtedly, tissue necrosis caused by coronary artery occlusion is one of the most common diseases of Western society, causing significant mortality and morbidity (Latet et al., 2015). MI results in necrotic cardiomyocytes releasing their intracellular contents, which act as danger signals that cause sterile inflammation (Zhang et al., 2015). In healthy mice and humans, CD4⁺ T cells specific for cardiac self-antigen α -myosin heavy chain (α MyHC) escape thymic negative selection and seed the

periphery, rendering the heart vulnerable to an autoimmune attack (Lv et al., 2011). Up to 30% of MI patients develop signs of humoral autoimmunity that is often self-limiting but can be accompanied by pericarditis. This percentage increases to 80% of autoimmune prone type I diabetes (T1D) patients. Non-obese diabetic (NOD) mice, a mouse model of T1D, also develop pathologic cardiac autoimmunity post MI, whereas wild-type (WT) C57BL/6 mice do not (Gottumukkala et al., 2012; Lipes and Galderisi, 2015). Environmental cues from an infarcted heart are thus sufficient to induce heart-specific immunity in autoimmune prone hosts in the absence of microbial ligands. It was hypothesized before that the innate inflammatory response in the infarcted heart can initiate the maturation of DCs, licensing them for activation of T cells directed against the heart (Gottumukkala et al., 2012; Lv and Lipes, 2012); however, direct evidence of this DC-T cell interaction post MI is lacking. To study if danger signals released by tissue injury can activate DCs and generate adaptive immunity, TCR transgenic mice (TCR-M) have been developed to measure CD4⁺ T cell responses to α MyHC (Nindl et al., 2012). Using these tools, we studied if, where, and how cardiac self-antigens are presented. In steady state, conventional type 1 DCs (cDC1s) presented cardiac self-antigen to α MyHC-specific TCR-M cells only in heart-draining mediastinal lymph nodes, leading to Treg expansion. In mice in which MI was induced, cardiac DCs were activated and in vivo α MyHC presentation was increased. Post MI, mainly conventional type 2 DCs (cDC2s) presented α MyHC and induced the formation of interferon (IFN) γ - and interleukin (IL)-17-producing TCR-M cells. These findings show that tissue necrosis activates autoreactive T cells through DC maturation and migration.

RESULTS

CD11c-Expressing Cells in the Heart Can Be Subdivided into cDC1s, cDC2s, and moDCs

Conventional DCs, which form the crucial link between innate and adaptive immunity, are divided into two subsets termed cDC1s and cDC2s (Guilliams et al., 2014). cDCs arise in a Flt3L-dependent manner from progenitors in the bone marrow (Waskow et al., 2008), and are divided based on surface markers and differential dependence on transcription factors (TFs) (Sichien et al., 2017). cDC1s express XCR1 and CD103 and depend on Batf3 and IRF8, whereas cDC2s express CD172 α (SIRP α) and CD11b and partially depend on Zeb2 and IRF4 (Bajaña et al., 2012; Scott et al., 2016). Because DC subsets in the murine heart are poorly defined, we characterized subsets in the healthy heart. We used flow cytometry to identify CD11c⁺ cells among live non-autofluorescent CD45⁺ Lineage⁻ cells. These were further divided based on MHCII and CD64 to identify MHCII⁺CD64⁻ cDCs and CD64⁺MHCII⁺ monocyte-derived DCs (moDCs) (Figure 1A). Embryonically derived macrophages (MFs) were outgated because these cells are autofluorescent and do not express CD11c (Molawi et al., 2014; Epelman et al., 2014). cDCs can be further subdivided into XCR-1⁺ cDC1s and CD172 α ⁺ cDC2s, whereas moDCs uniformly expressed CD172 α . CD11c⁺ cells made up 0.98% \pm 0.27% (mean \pm SEM) of all living heart cells and 7.39% \pm 1.36% of CD45⁺ leukocytes. cDC1s and cDC2s made up 4.77% \pm 0.16% and 14.5% \pm 1.25% of

total CD11c-expressing cells, respectively, whereas 16.87% \pm 3.09% of CD11c⁺ cells were moDCs (Figures 1B and 1C). cDC development depends on Flt3L, whereas moDC development does not (Waskow et al., 2008). So to confirm cDC and moDC identification, hearts of *Flt3l*^{-/-} mice were compared with *Flt3l*^{+/+} hearts. We found a severe reduction in cDC1s and cDC2s in the *Flt3l*^{-/-} heart compared with WT mice, whereas moDCs were unaffected (Figures 1D and 1E), demonstrating that only heart cDCs are Flt3L dependent. We next examined the expression of surface markers associated with DC subsets (Figures 1F and 1G). Cardiac cDC subsets expressed the typical cDC markers CD26 (Miller et al., 2012) and Flt3. As described in other tissues, cDC2s and moDCs expressed CD11b, whereas cDC1s expressed CD103. cDC1s uniformly expressed CD24, whereas cDC2s were separated into CD24⁺ and CD24⁻ cDC2s, as described for lung cDC2s (Bajaña et al., 2016). Expression of CADM1, a universal cDC1 marker (Guilliams et al., 2016; Gurka et al., 2015), was restricted to cDC1s. MoDCs expressed the typical MF markers MerTK, Mar-1, and F4/80, although some F4/80 expression was also noted on cDC2s, as found in other tissues (Tamoutounour et al., 2013). As expected, moDCs expressed CCR2, which is critical for monocyte exit from the bone marrow. CCR2 was also expressed on cDCs, as observed in intestinal cDC2s (Scott et al., 2015).

We next FACS-purified cDC1s, cDC2s, moDCs, and CD11c⁻ MFs from a steady-state heart and performed RNA-sequencing (RNA-seq) analysis (Figures 1H and 1I). To confirm identification of heart cDC1s and cDC2s, we generated a list of hallmark genes across a range of tissues by examining the transcriptomes of cDC subsets available from the Immgen consortium. Gene expression in cardiac APC populations was then studied. Cardiac cDC1s indeed expressed cDC1 genes, including *Clec9a*, *Cadm1*, *Itgae*, *Tlr3*, and *Irf8*, whereas these genes were lowly expressed by cardiac cDC2s, moDCs, and MFs (Figure 1H). cDC2 genes like *Cd11b*, *Cd72*, *Csf1r*, *Zeb2*, and *Irf4* were highly expressed by cardiac cDC2s compared with cDC1s (Figure 1I). Taken together, these data highlight the previously unappreciated heterogeneity among cardiac DCs.

Transcription Factor Dependency of Cardiac cDC Subsets

The molecular requirements for cardiac DC development have been poorly studied. Because cDC1s and cDC2s in other tissues are thought to depend on IRF8 and IRF4, respectively (Mildner and Jung, 2014), we hypothesized that this would be the same for cardiac cDCs. Therefore, we first examined IRF8 and IRF4 expression in cardiac DCs at the protein level (Figures 2A and 2B). IRF4 was most highly expressed by cardiac cDC2s, whereas cDC1s expressed high levels of IRF8. Next, we crossed mice expressing CRE recombinase under the control of the CD11c promoter (*Cd11cCre* mice) (Caton et al., 2007) with *Irf4*^{fllox} (Persson et al., 2013) or *Irf8*^{fllox} mice (Sichien et al., 2016) to generate mice lacking IRF4 or IRF8 expression, respectively, in CD11c⁺ cells. Whenever CRE was expressed in CD11c⁺ cells, *Irf4* or *Irf8* was efficiently floxed out and their protein levels declined (data not shown). Analysis of *Irf4*^{fl/fl}*Cd11cCre* mice revealed that cardiac cDC2 (CD172 α ⁺CD24^{+/-}) were only slightly reduced (Figures 2C and 2E). However, a significant reduction

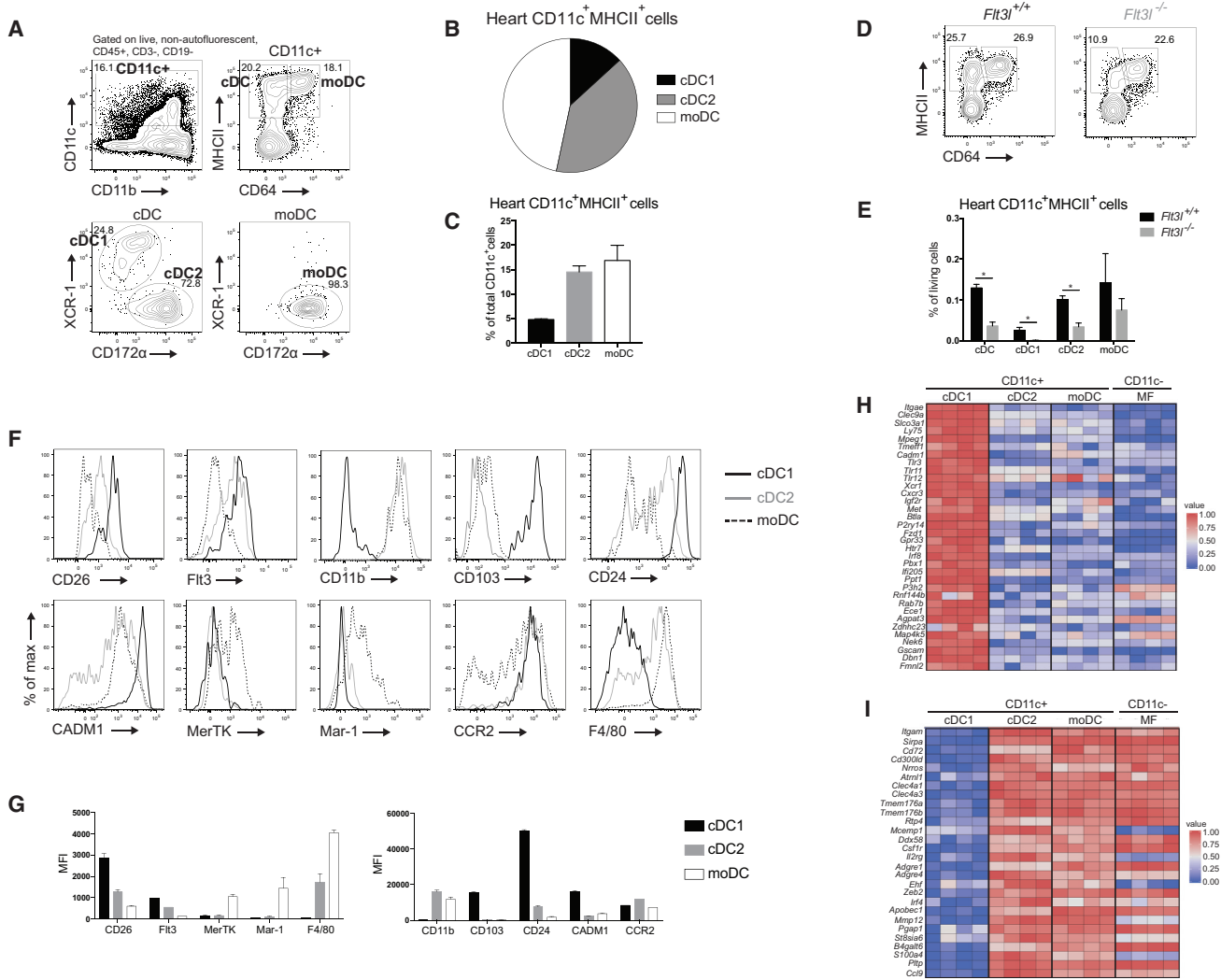


Figure 1. CD11c-Expressing Cells in the Heart Can Be Subdivided into cDC1s, cDC2s, and moDCs

(A) Flow cytometry gating strategy for DC subsets in steady-state heart of WT mice.
 (B) Pie chart representing the distribution of DC subsets in naive murine WT heart.
 (C) DC subset percentages of total CD11c⁺ cells in naive heart of WT mice.
 (D) Expression of MHCII and CD64 in CD45⁺Lineage⁻CD11c⁺ cells from naive heart in *Fit3*^{+/+} and *Fit3*^{-/-} mice.
 (E) Total cDC, cDC1, cDC2, and moDC percentages of total living cells in naive heart of *Fit3*^{+/+} and *Fit3*^{-/-} mice.
 (F) Representative histograms of CD26, *Fit3*, CD11b, CD103, CD24, CADM1, MerTK, Mar-1, CCR2, and F4/80 expression in steady-state WT heart cDC1s, cDC2s, and moDCs (n = 3).
 (G) MFI of marker expression on steady-state WT heart DC subsets shown in (F).
 (H and I) Heat map of relative expression of (H) hallmark cDC1 genes and (I) hallmark cDC2 genes in cDC1s, cDC2s, moDCs, and MFs sorted from naive WT hearts acquired by RNA-seq. All data in Figure 1 represent at least two independent experiments, and all bar graphs show data as mean ± SEM (*p < 0.05).

in CD24⁺ cDC2s was observed, suggesting that IRF4 is important for their terminal differentiation, as described in the lung (Bajaña et al., 2016). Because IRF4 has also been implicated in regulating cDC2 migration (Bajaña et al., 2012), we next studied cDC2 frequency in the heart-draining mediastinal lymph node (mLN) (Figures 2D and 2E). Migration of both CD24⁺ and CD24⁻ cDC2s was indeed lower in the mLN of *Irf4*^{fl/fl}.*Cd11c*Cre mice. Examination of cDC subsets in the heart and mLN of *Irf8*^{fl/fl}.*Cd11c*Cre mice demonstrated an almost complete abla-

tion of cDC1s (CD24⁺CD172a⁻) in both locations (Figures 2F–2H). cDC2s were unaffected in the *Irf8*^{fl/fl}.*Cd11c*Cre heart, but were significantly increased in the mLN. Thus, cardiac cDC1s and cDC2s, similarly to their counterparts in other organs, depend on IRF8 and IRF4, respectively, for their development (cDC1s and CD24⁺ cDC2s) and migration to the lymph nodes (LNs) (cDC2s). Thus, *Irf8*^{fl/fl}.*Cd11c*Cre and *Irf4*^{fl/fl}.*Cd11c*Cre mice represent two models in which cardiac cDC1 and cDC2 function, respectively, can be assessed.

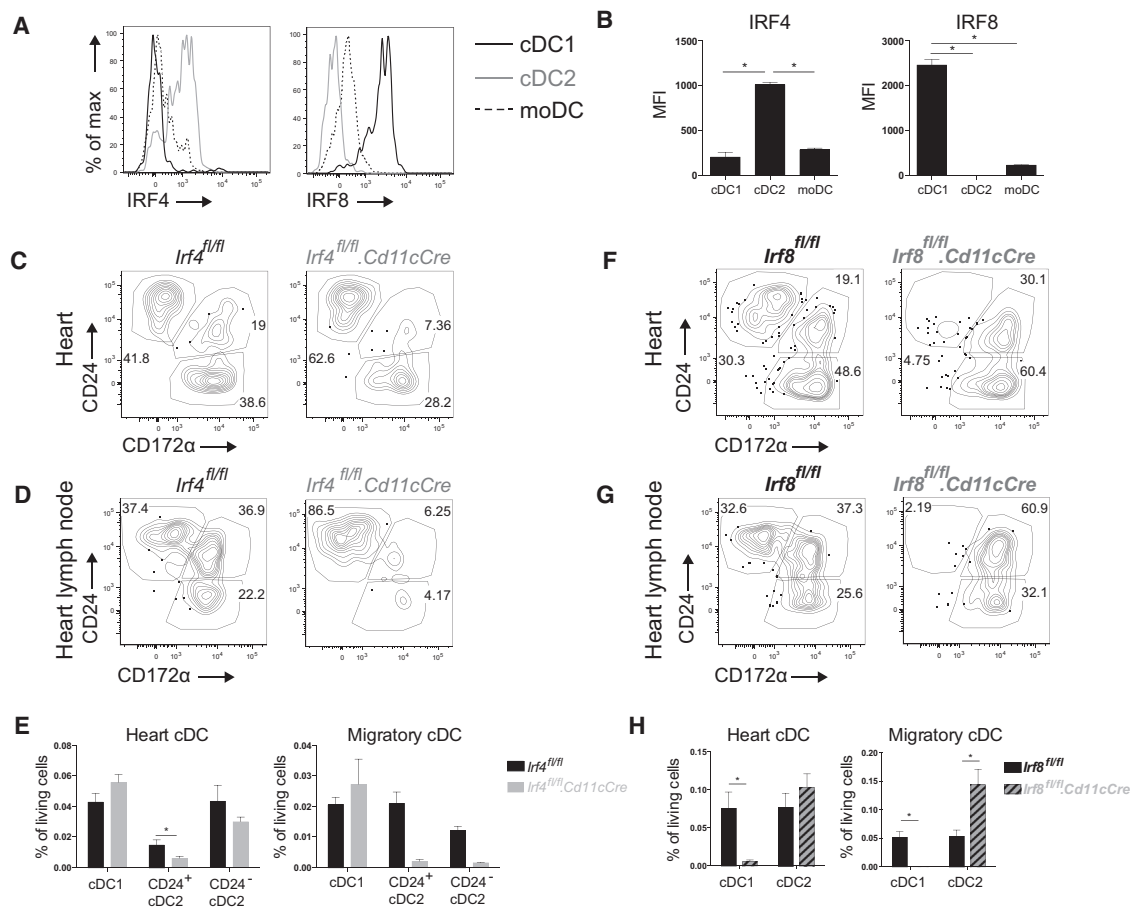


Figure 2. Transcription Factor Dependency of Cardiac cDC Subsets

(A) Representative histogram of IRF4 and IRF8 expression of steady-state WT heart cDC1s, cDC2s, and moDCs. (B) MFI of IRF4 and IRF8 expression on naive WT heart DC subsets shown in (A). (C and D) MHCII⁺CD11c⁺CD64⁻ cDCs are divided into CD24⁺CD172α⁻ cDC1s, CD24⁺CD172α⁺ cDC2s, and CD24⁻CD172α⁺ cDC2s in *lrf4^{fl/fl}* and *lrf4^{fl/fl}.Cd11cCre* steady-state heart (C) and mediastinal LN (D). (E) Percentage of living cells of cDCs in *lrf4^{fl/fl}* and *lrf4^{fl/fl}.Cd11cCre* naive heart and mLN. (F and G) MHCII⁺CD11c⁺CD64⁻ cDCs are divided into CD24⁺CD172α⁻ cDC1s, CD24⁺CD172α⁺ cDC2s, and CD24⁻CD172α⁺ cDC2s in *lrf8^{fl/fl}* and *lrf8^{fl/fl}.Cd11cCre* steady-state heart (F) and mLN (G). (H) Percentage of living cells of cDCs in *lrf8^{fl/fl}* and *lrf8^{fl/fl}.Cd11cCre* steady-state heart and mLN. All data in Figure 2 represent at least two independent experiments, and all bar graphs show data as mean ± SEM (*p ≤ 0.05).

IRF8-Dependent cDC1s Generate Myosin-Specific Tregs in Heart-Draining Lymph Node

Although the heart is not continuously exposed to environmental antigens compared with mucosal surfaces, heart DCs can encounter cardiac self-antigens, such as α-myosin heavy chain (αMyHC). Because αMyHC autoreactive CD4⁺ T cells escape from the thymus into the periphery (Lv et al., 2011), it is plausible that cardiac DCs would function in preserving peripheral tolerance to the heart. Thus, we next examined if cardiac cDC1s or cDC2s played such a role. A critical tool to answer this key question was αMyHC-specific TCR-M mice (Nindl et al., 2012). Naive CD62L⁺CD44⁻CD4⁺ T cells were purified from TCR-M splenocytes, CFSE labeled, and injected into steady-state WT littermates (*lrf4^{fl/fl}* and *lrf8^{fl/fl}* mice without *Cd11cCre* expression) to determine if and where αMyHC is presented. Various lymphoid organs of acceptor mice were collected for analysis 3 days after

TCR-M transfer. Undivided TCR-M cells were present in all organs examined, consistent with the migratory behavior of naive T cells (Figures 3A and 3D). TCR-M proliferation detected by CFSE dilution and CD44 expression was exclusively observed in the heart-draining mediastinal LN of naive WT mice. TCR-M proliferation and activation in mLN demonstrated αMyHC transport and presentation without the presence of cardiac damage (Figures 3B and 3E). Upon division, TCR-M cells gained expression of T-bet and RoRγt, respectively, and TFs for Th1 and Th17 cells (Figures 3C and 3F). Divided cells also expressed Foxp3 and CD25 indicative for Tregs (Figures 3C and 3F). To verify if migratory cDC2s were responsible for αMyHC presentation in mLN, naive TCR-M cells were injected in *lrf4^{fl/fl}.Cd11cCre* mice. TCR-M cells in *lrf4^{fl/fl}.Cd11cCre* mLN proliferated equally well as in WT littermates, indicating that cDC2 migration is not necessary for αMyHC presentation (Figures 3A and 3B). T-bet,

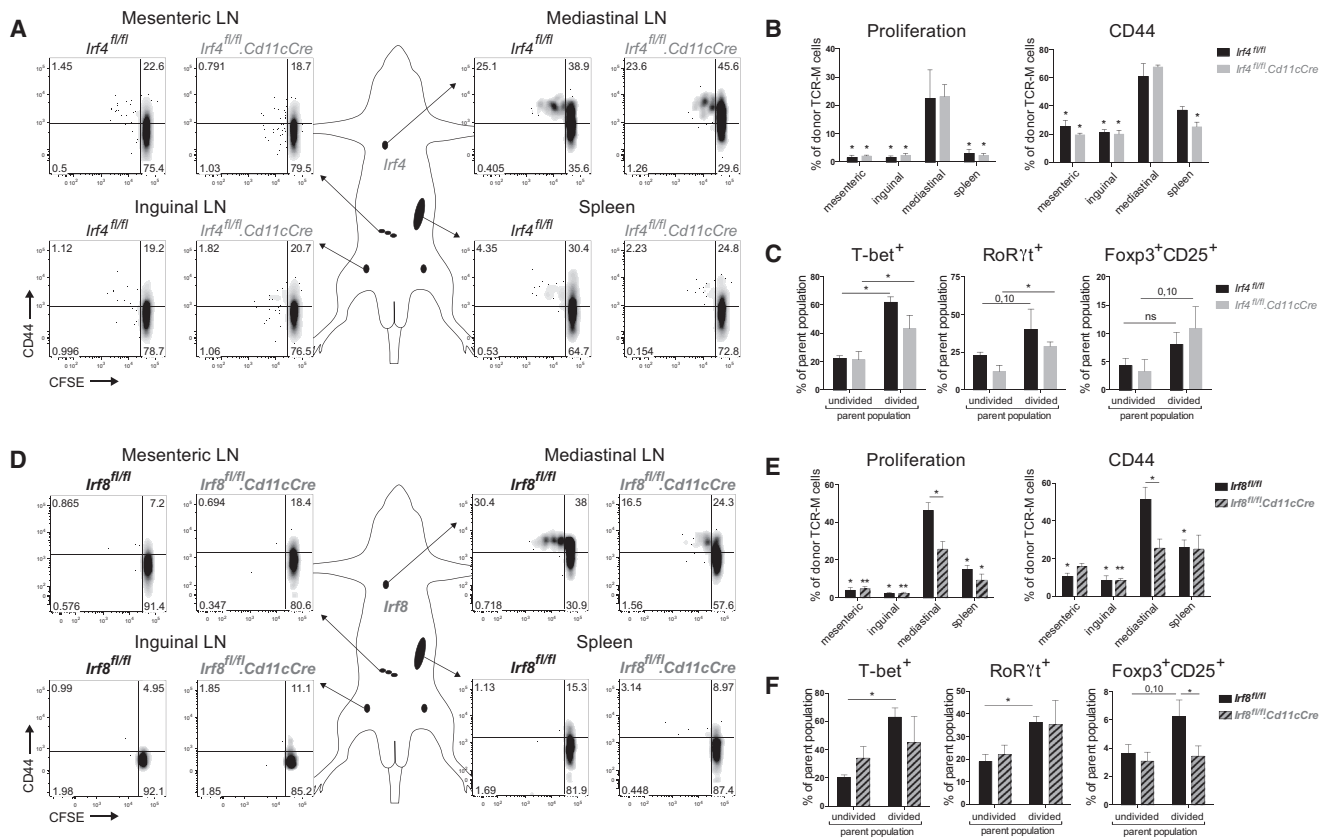


Figure 3. IRF8-Dependent cDC1s Generate Myosin-Specific Tregs in Heart-Draining Lymph Node

(A) Depicted LNs and spleen were isolated from TCR-M acceptor *Lrf4*^{fl/fl} and *Lrf4*^{fl/fl}.*Cd11cCre* mice 3 days after naive TCR-M transfer. CFSE dilution and CD44 expression of donor TCR-M cells was analyzed by flow cytometry. (B) Percentage of proliferation and CD44 expression of donor TCR-M cells in LNs and spleen from the experiment described in (A) (n = 4). (C) Percentage of T-bet, RoRyt, and Foxp3/CD25 expression on undivided and divided donor TCR-M cells isolated from mLN in *Lrf4*^{fl/fl} and *Lrf4*^{fl/fl}.*Cd11cCre* steady-state mice (n = 4). (D) 3 days after naive TCR-M injection, depicted LNs and spleen were isolated from TCR-M acceptor *Lrf8*^{fl/fl} and *Lrf8*^{fl/fl}.*Cd11cCre* mice. CFSE dilution and CD44 expression of donor TCR-M cells was analyzed by flow cytometry. (E) Percentage of proliferation and CD44 expression of donor TCR-M cells in LNs and spleen from the experiment described in (D) (n = 5). (F) Percentage of T-bet, RoRyt, and Foxp3/CD25 expression on undivided and divided donor TCR-M cells isolated from mLN in *Lrf8*^{fl/fl} and *Lrf8*^{fl/fl}.*Cd11cCre* steady-state mice (n = 5). All data in Figure 3 represent at least three independent experiments, and bar graphs show data as mean ± SEM (*p ≤ 0.05).

RoRyt, and Foxp3 increase upon division was unchanged in *Lrf4*^{fl/fl}.*Cd11cCre* mLN compared with *Lrf4*^{fl/fl} (Figure 3C). Naive TCR-M cells were next administered to *Lrf8*^{fl/fl}.*Cd11cCre* mice to study if cDC1s were responsible for steady-state α MyHC presentation. Proliferation and CD44 expression was significantly lower in mLN of *Lrf8*^{fl/fl}.*Cd11cCre* mice compared with *Lrf8*^{fl/fl} mice 3 days post-transfer (Figures 3D and 3E). Although T-bet and RoRyt upregulation in divided TCR-M cells was not altered in *Lrf8*^{fl/fl}.*Cd11cCre* mLN (Figure 3F), Foxp3 induction was significantly reduced in divided TCR-M cells from *Lrf8*^{fl/fl}.*Cd11cCre* mLN, showing a block in iTreg generation in the absence of cDC1s. Our findings identify cardiac cDC1s as necessary for α MyHC-specific Treg induction from naive TCR-M cells.

DCs Infiltrate the Heart and Migrate to the Mediastinal Lymph Node Following MI

MI triggers an inflammatory response characterized by infiltration of innate immune cells (Latet et al., 2015). Although infiltra-

tion of DCs has been described in infarcted hearts (Maekawa et al., 2009), DC subsets have not been identified. Thus, we first sought to characterize DC subsets post MI. We induced MI in WT female mice by permanently ligating the left anterior descending (LAD) coronary artery and examined DCs at various time points post-surgery. Consistent with previous reports, the proportion of CD11c⁺ cells was increased compared with sham-operated controls (Figure 4A). A significant part of CD11c⁺ cells in MI hearts was CD64⁺MHCII⁻. These cells were not further analyzed because they lacked MHCII expression. They are probably MFs recruited due to MI, as seen in other sterile inflammation models (Zigmond et al., 2014). At day 7 post-surgery, we also observed a dramatic increase in moDCs (CD64⁺CD172 α ⁺) in MI hearts compared to sham (Figures 4A and 4B). Analysis of DC subsets between 2 and 10 days post MI revealed an increase of all subsets by day 2 post MI, with the peak of XCR-1⁺ cDC1 and moDC infiltration at day 7. CD172 α ⁺ cDC2 numbers peaked at day 5 post MI. moDCs contributed most to the total infarcted heart

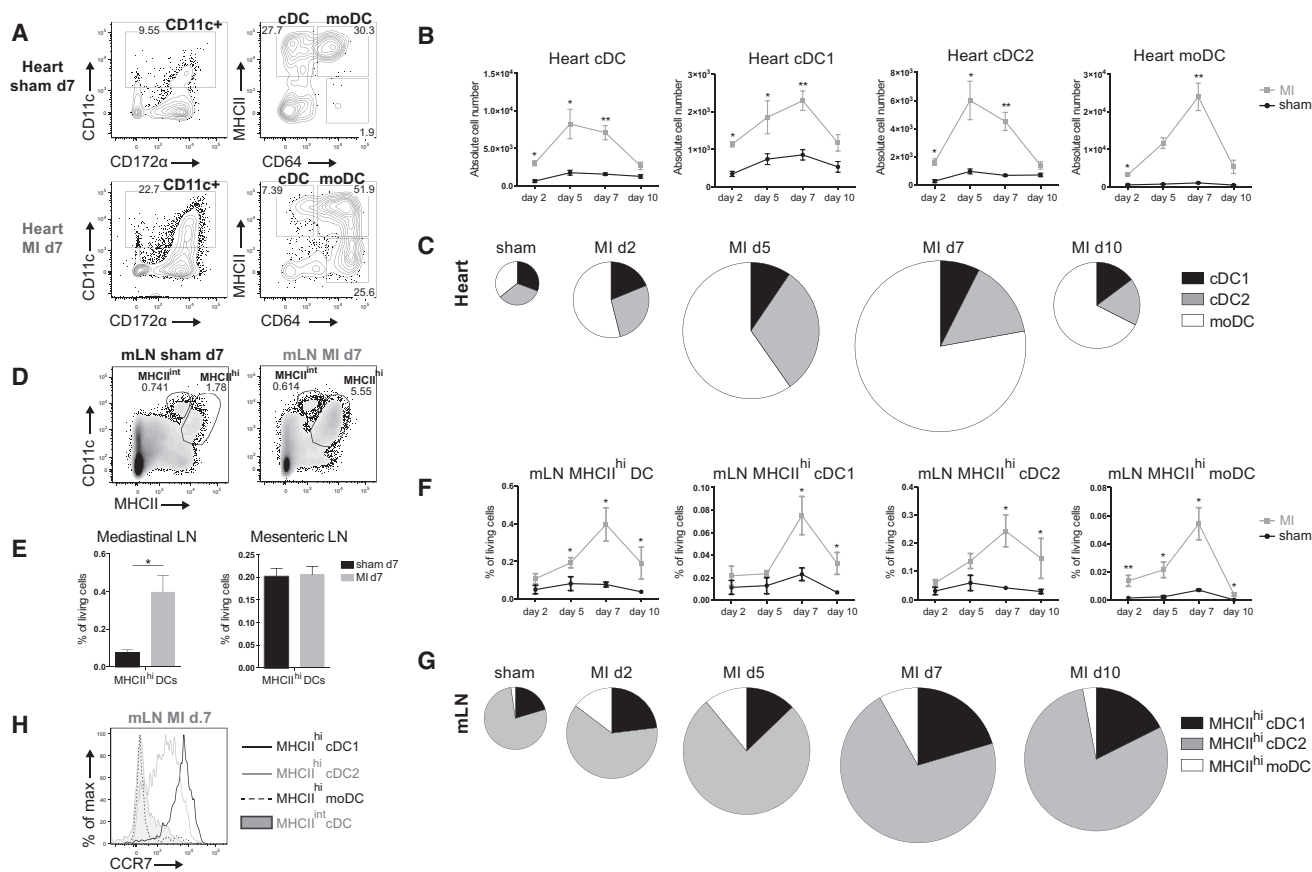


Figure 4. DCs Infiltrate the Heart and Migrate to Mediastinal Nodes Following MI

(A) Representative gating strategy for DC subsets in the heart of sham-operated and infarcted WT mice on day 7 post-surgery. (B) Absolute cell numbers of DC subsets in the heart of sham-operated and infarcted mice on day 2, 5, 7, and 10 post-surgery ($n = 3-6$). (C) Pie charts depicting the distribution of DC subsets in the sham-operated heart (pooled data from day 2-5-7-10 post-surgery) and infarcted heart on day 2, 5, 7, and 10 post-MI. Pie chart sizes are proportional to total cardiac DC percentages. (D) Representative gating strategy for MHCII^{int} and MHCII^{hi} DCs in mediastinal LN of sham-operated and infarcted WT mice on day 7 post-surgery. (E) MHCII^{hi} DC percentages of total living cells in mediastinal and mesenteric LN in sham-operated and infarcted mice at day 7 post-surgery ($n = 6$). (F) MHCII^{hi} DC subset percentages of total living cells in mediastinal LN of sham-operated and infarcted mice on day 2, 5, 7, and 10 post-surgery ($n = 3-6$). (G) Pie chart illustrating distribution of cDC1s, cDC2s, and moDCs among total MHCII^{hi} DC population in mLN in sham-operated and infarcted mice at day 2, 5, 7, and 10 post-surgery. Pie chart sizes are proportional to total MHCII^{hi} DCs in mLN. (H) Representative histogram of CCR7 expression of MHCII^{hi} cDC1s, MHCII^{hi} cDC2s, MHCII^{hi} moDCs, and MHCII^{int} cDCs from mLN on day 7. All bar graphs in Figure 4 show data as mean \pm SEM ($*p \leq 0.05$; $**p \leq 0.01$), and all data are representative of two independent experiments.

DC population. All subsets returned to near baseline levels within 10 days (Figures 4B and 4C). Next, we studied migration to the heart-draining mediastinal LN post MI. Typically, DCs that have migrated to the LN from the periphery are MHCII^{hi}, in contrast to LN-resident DCs that are MHCII^{int}. An increase in MHCII^{hi} DCs was observed in mediastinal, but not mesenteric, LNs 7 days post MI compared with sham (Figures 4D and 4E). Among MHCII^{hi} DCs, we identified XCR-1⁺ cDC1s, CD172 α ⁺ cDC2s, and CD64⁺ moDCs. We followed DC migration to the mediastinal LN between 2 and 10 days post-surgery (Figures 4F and 4G). Consistent with heart DC infiltration, MHCII^{hi} DC subsets peaked at day 7 post MI. MHCII^{hi} cDC2s represented the largest DC population. To validate if DCs had indeed migrated from the heart, we examined CCR7 expression, the chemokine receptor required for migration to the LN (Ohl et al., 2004). As expected,

MHCII^{hi} cDC1s and cDC2s expressed CCR7 and hence migrated to the LN, whereas MHCII^{int} cDCs lacked CCR7 (Figure 4H). However, MHCII^{hi} moDCs did not express CCR7, suggesting that moDCs have not migrated from the heart and instead have merely upregulated MHCII, as has been reported (Tamoutounour et al., 2013).

DCs from Infarcted Heart Have an Activated Phenotype

To gain more insight in the phenotype of DCs infiltrating the infarcted heart, we performed RNA-seq on heart cDC1s, cDC2s, and moDCs sorted from post MI day 7 hearts. As a reference population, we also sorted cardiac CD11c⁻ MFs (Lineage⁻CD11c⁻MHCII⁺CD64⁺CD172 α ⁺). Unsupervised principle-component analysis (PCA) showed that irrespective of the heart tissue environment (steady state or MI), cardiac DCs clustered

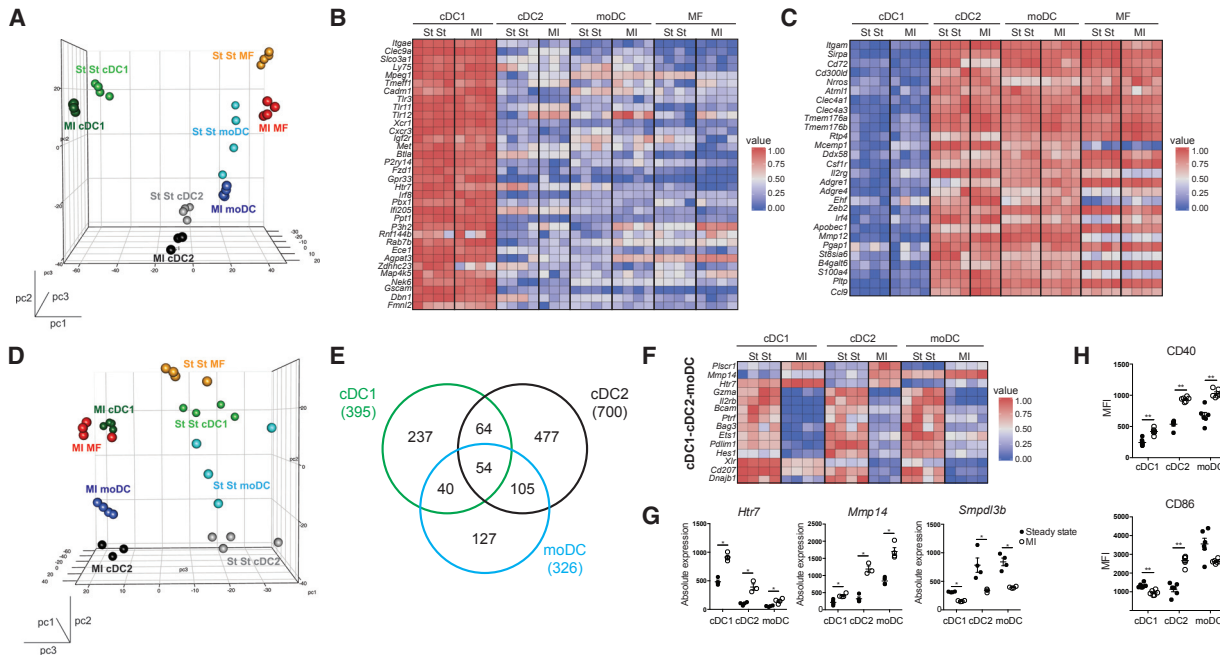


Figure 5. DCs from Infarcted Heart Have an Activated Phenotype

(A) Front view of PCA of RNA-seq data from cDC1s, cDC2s, moDCs, and MFs in the steady-state (St St) and the infarcted (MI d7) heart. PCA was calculated using the top 15% most varying genes between cell subsets. Each dot symbolizes one independently sorted replicate of the indicated cell population, and four independent sorts were performed per subset.

(B and C) Heat map of relative expression of hallmark cDC1 genes (B) and hallmark cDC2 genes (C) in cDC1s, cDC2s, moDCs, and MFs sorted from steady-state and infarcted hearts.

(D) Side view of PCA of RNA-seq data from cDC1s, cDC2s, moDCs, and MFs in the steady-state and infarcted heart.

(E) Venn diagram showing numbers and overlap of DEGs in cDC1s, cDC2s, and moDCs sorted from MI d7 compared to steady-state hearts.

(F) Heat map of relative expression of top-shared DEGs between DC subsets from MI d7 hearts compared to corresponding subsets isolated from the steady-state heart. To calculate top DEGs, a threshold of a minimum 1.5 Log₂ fold change was used. As an exception, no threshold was set on shared upregulated genes of cDC1s, cDC2s, and moDCs.

(G) Bar graphs representing absolute expression of DEGs among cDC1s, cDC2s, and moDCs sorted from steady-state and infarcted hearts.

(H) MFI of CD40 and CD86 expression (day 7 post-surgery) on heart DC subsets in sham-operated compared to the infarcted heart (n = 6). All bar graphs in Figure 5 show data as mean ± SEM (*p ≤ 0.05; **p ≤ 0.01), and all data are representative of four independent experiments. See also Figure S1 and Tables S1–S7.

by subset on principal components 1 (pc1) and 2 (pc2) (Figure 5A). Also, expression of hallmark cDC1 (Figure 5B) and cDC2 genes (Figure 5C) did not change in cardiac DCs post MI. Interestingly, pc3 divided cell subsets into two groups, those deriving from the steady state or infarcted heart (Figure 5D), suggesting a global MI signature, which was conferred upon the subsets post MI. To further examine the MI signature, gene expression of infarcted heart DCs was compared with that of steady-state heart DCs to identify differentially expressed genes (DEGs). We found that 395, 700, and 326 genes were differentially expressed in cDC1s, cDC2s, and moDCs, respectively, between healthy and infarcted hearts (Figure 5E; Tables S1–S3). To determine the global MI signature, we assessed which DEGs were conserved between DC subsets and found that 54 genes were differentially expressed in the three DC subsets (Figures 5E and 5F; Table S4). Analysis of these 54 genes suggested that DC subsets would be altered in their activation status. *Htr7* (encoding serotonin receptor 5-HT₇R) and *Mmp14* (encoding metalloproteinase MMP-14) were both upregulated in MI and are linked to DC migration (Figures 5F and 5G; complete DEG lists can be found in the Supple-

mental Information; Tables S5–S7) (Holst et al., 2015; Gawden-Bone et al., 2010). *Smpd13b* (encoding sphingomyelin phosphodiesterase, acid-like 3B) was downregulated and encodes a negative regulator of TLR signaling (Heinz et al., 2015), suggesting increased TLR signaling in post MI DCs. Recently, several gene clusters were found to be induced upon homeostatic or TLR-induced cDC1 maturation (Ardouin et al., 2016). We observed that cDC1s from MI hearts were enriched for genes upregulated by TLR-induced maturation, suggesting that cDC1s in infarcted hearts were indeed induced to mature in a TLR-dependent manner (Figures S1A and S1D). cDC2s and moDCs from MI hearts were enriched in genes upregulated by TLR-induced and homeostatic maturation (Figures S1B and S1D).

To determine if DCs were also activated at the protein level post MI, expression of the activation markers CD40 and CD86 was examined by flow cytometry during the peak of DC infiltration (day 7). As predicted by RNA-seq, the ischemic environment induced DC activation. All DC subsets showed increased expression of CD40 post MI (Figure 5H). However, CD86 expression was only increased on cDC2s from infarcted hearts.

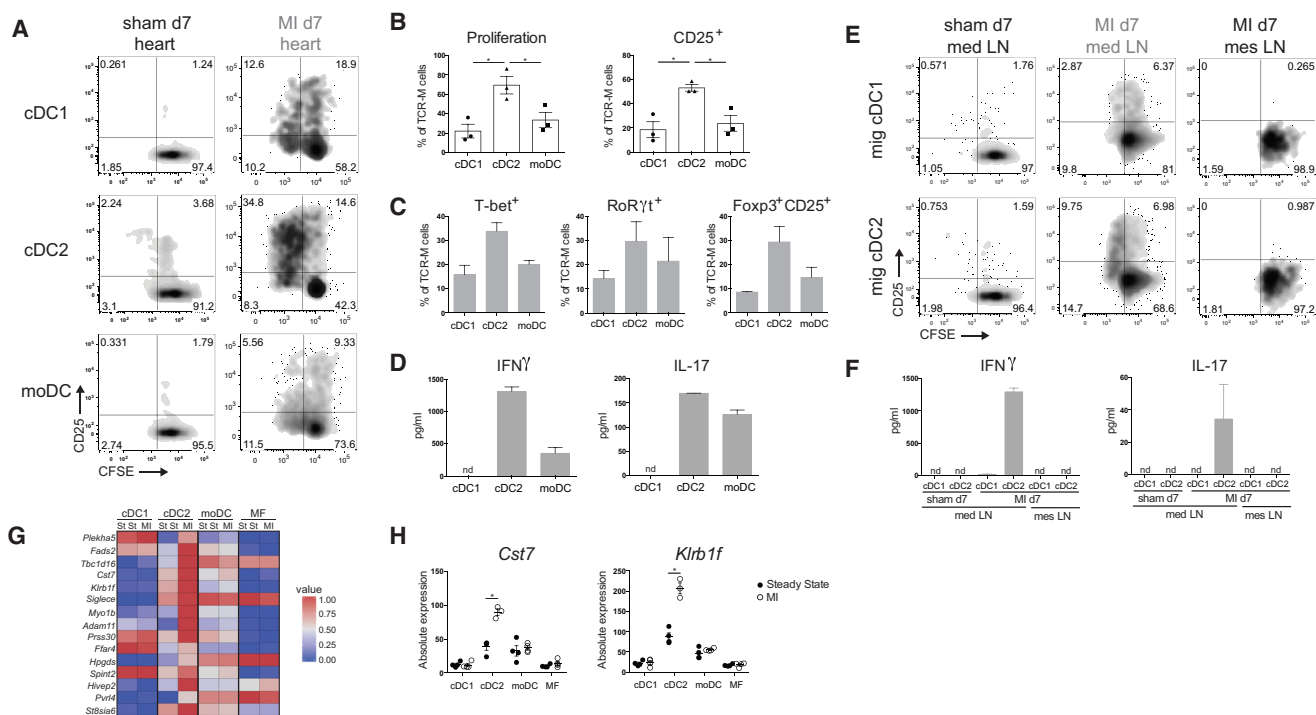


Figure 6. cDC2s Are the Main Presenters of α MyHC to Effector Autoreactive CD4⁺ T Cells Ex Vivo

(A) CFSE dilution and CD25 expression of TCR-M cells in co-culture with sorted heart DC subsets from sham-operated versus MI d7 mice. Data are representative of three independent experiments (n = 12).

(B) Quantification of percentages of proliferated and CD25-expressing TCR-M cells from co-cultures plotted in (A). Individual dots represent the value of one independent experiment (mean \pm SEM; *p \leq 0.05).

(C) Percentage of T-bet, RoR γ t, and Foxp3/CD25 expression on TCR-M cells co-cultured with sorted heart DC subsets from MI day 7 hearts (mean \pm SEM).

(D) In supernatants of co-cultures plotted in (A), cytokines produced by TCR-M cells were detected by ELISA. Mean is calculated from values of technical replicates from one experiment (nd, not detectable) (mean \pm SD).

(E) CFSE dilution and CD25 expression of TCR-M cells co-cultured with sorted migratory cDC1s and cDC2s from mLNs of sham-operated and MI mice and from mesenteric LNs of MI mice.

(F) After 3 days of co-culture (plotted in E), cytokines were measured in supernatants by ELISA. Mean is calculated from values of technical replicates from one experiment (nd, not detectable) (mean \pm SD).

(G) Heat map of relative expression of cDC2 genes exclusively upregulated in cDC2s from the infarcted heart compared to steady state.

(H) Bar graphs representing absolute expression of interesting unique cDC2 DEGs (mean \pm SEM; *p \leq 0.05).

See also [Table S8](#).

cDC2s Are the Main Presenters of α MyHC to Effector Autoreactive CD4⁺ T Cells Ex Vivo

Having shown that DCs infiltrate the heart, adopt an activated phenotype post MI, and migrate to mLNs, we next examined if they presented the cardiac self-antigen α MyHC, released from necrotic cardiomyocytes to autoreactive T cells. To this end, we sorted cDC1s, cDC2s, and moDCs from the heart at day 7 post MI and sham controls and co-cultured them ex vivo with TCR-M cells. Consistent with cDC2s being superior at presenting antigen to CD4⁺ T cells and with their mature state post MI, proliferation and activation of TCR-M cells was increased when co-cultured with cDC2s from MI hearts compared with cDC1s and moDCs (Figures 6A and 6B). Nonetheless, cDC1s and moDCs from the MI heart induced more TCR-M proliferation compared to subsets from the sham heart (Figure 6A). Fitting with the highest proliferation, TCR-M cells cultured with heart cDC2s post MI exhibited increased expression of T-bet, RoR γ t, and Foxp3 (Figure 6C) and the highest

IFN γ and IL-17 production (Figure 6D). Migratory cDC2s sorted from mLNs 7 days post MI were similarly best at inducing TCR-M proliferation, whereas migratory cDC1s only activated TCR-M cells (Figures 6E and 6F). Importantly, neither migratory cDCs from sham mLNs nor migratory cDCs from mesenteric LNs post MI stimulated TCR-M cells. To look further into the mechanisms of cDC2 superiority, we returned to our RNA-seq analysis. Using a stringent cut off described in the [Supplemental Experimental Procedures](#), the list of cDC2 DEGs (MI compared to steady state) was reduced from 477 to 31 ([Table S8](#)). 15 DEGs were upregulated (Figure 6G), including *Cst7* (encoding cystatin F) and *Klrb1f* (encoding killer cell lectin-like receptor subfamily B member 1F) (Figure 6H), which encode proteins involved in antigen processing on MHCII (Magister et al., 2012) and T cell stimulation, respectively (Tian et al., 2005). This provides a plausible mechanism for the increased ability of cDC2s from the infarcted heart to present α MyHC to TCR-M cells.

Myocardial Infarction Activates Autoreactive CD4⁺ T Cells In Vivo

Having shown that MI induces cardiac self-antigen presentation by DCs *ex vivo*, we next sought to examine if MI would activate autoreactive T cells *in vivo*. Therefore, naive TCR-M cells were transferred to MI and sham mice 2 and 7 days post-surgery and proliferation was analyzed 3 days later. TCR-M proliferation was increased in mLN of mice injected at day 2 post MI compared with sham, *in vivo* demonstrating increased α MyHC presentation early post MI (Figures 7A and 7B). TCR-M cells transferred to mice at day 2 post MI did not upregulate CD25 and Foxp3 Treg markers in mLN compared to sham mLN (Figure 7C). This suggests that iTreg differentiation was blunted after MI, potentially leading to a break in self-tolerance to the heart. Remarkably, TCR-M cells also proliferated in non-heart-draining lymphoid organs like the spleen and mesenteric LNs of MI mice compared with sham at day 2 (Figures 7A and 7B). This could suggest early systemic release of α MyHC post MI, which is presented by cDCs in non-draining lymphoid organs. Alternatively, divided TCR-M cells in non-draining LNs could be recirculating TCR-M cells that originally divided in mLN. To address this, an *ex vivo* co-culture was set up with bulk LN cells from sham d2, MI d2, and MI d7 mice as the antigen source and naive TCR-M cells as the readout for antigen presence (Figure 7D). TCR-M cells exclusively proliferated in the presence of mLN cells from MI d2 and d7 mice and not with mesenteric LN and spleen cells, suggesting that α MyHC is not systemically released in sufficiently high amounts post MI to stimulate TCR-M cells in this *in vitro* setting.

Presentation of Cardiac Myosin in the Absence of cDC Subsets following MI

Having demonstrated that self-antigen is presented to autoreactive T cells both *ex vivo* and *in vivo*, with cDC2s appearing to be specialized in this, we next set out to determine which cDC subsets were necessary and/or sufficient for presenting α MyHC post MI. We opted to use *Irf4^{fl/fl}.Cd11cCre* and *Irf8^{fl/fl}.Cd11cCre* mice. Although loss of IRF4 did not decrease cDC2 populations in the sham and MI heart, migratory cDC2s in the mLNs were significantly reduced (Figure 7E); thus, these mice could be used to assess the role of migratory cDC2s post MI. Naive TCR-M cells were then transferred to *Irf4^{fl/fl}.Cd11cCre* mice 2 days post MI. Intriguingly, decrease in migratory cDC2s in mLN of *Irf4^{fl/fl}.Cd11cCre* mice did not affect TCR-M proliferation and activation compared with *Irf4^{fl/fl}* mice (Figures 7F and 7G), demonstrating that cDC2s are not necessary. To examine if cDC1s are needed, we performed the same experiment in *Irf8^{fl/fl}.Cd11cCre* mice because they lack cDC1s in the heart and mLN in both sham and MI mice (Figure 7H and data not shown). cDC1 loss had little effect on TCR-M proliferation and activation (Figure 7I). Proliferation was slightly reduced compared with *Irf8^{fl/fl}* controls but was still ~80%. So neither cDC1s nor cDC2s are specifically required for the presentation of α MyHC to autoreactive CD4⁺ T cells post MI.

DISCUSSION

It is widely accepted that DCs play a role in both the regulation of peripheral tolerance and induction of autoimmunity. However,

the exact mechanisms that cause DC activation and hence break tolerance remain to be dissected. One proposed mechanism is the maturation of DCs by necrotic cells (Gallucci et al., 1999); however, because this study was performed *in vitro*, it remains unclear if and how tissue necrosis would contribute to the initiation of autoimmunity *in vivo*. In this study, we addressed this issue using MI as a model of tissue necrosis. Intracellular contents released from necrotic cardiomyocytes can behave like danger signals, resulting in a sterile inflammatory response (Zhang et al., 2015). Prior to profiling the effects of MI on cardiac DCs, we performed a comprehensive analysis of distinct DC populations during homeostasis. Similar to other tissues, the steady-state heart contains a population of CD11c⁺MHCII⁺ cells, which we termed DCs. Further analysis led us to conclude that heart DCs could be divided into two populations of conventional DCs, termed cDC1s and cDC2s (Guilliams et al., 2014), and a population CD64⁺CD11c⁺MHCII⁺, which we termed moDCs, in line with what these cells were called previously (Tamoutounour et al., 2013). There is considerable controversy surrounding the correct name for this latter population because it is unclear if they are a bona fide DC population or a type of macrophage (Guilliams et al., 2016; Wu et al., 2016). Indeed, moDCs did not migrate from the heart to the LN, a hallmark of genuine DCs. However, moDCs did induce CD4⁺ T cell proliferation in *ex vivo* co-cultures to the same extent as cDC1s and higher than CD11c⁻ MFs (data not shown). Principal component analysis of gene expression also demonstrated that moDCs segregate in between cDCs and MFs. Thus, the exact nature and nomenclature of these cells remains unclear.

Because α MyHC-specific autoreactive CD4⁺ T cells escape the thymus, peripheral tolerance is essential to prevent a cardiac autoimmune attack (Lv et al., 2011). Although cardiac DCs have been proposed to play a role in self-tolerance (Hart and Fabre, 1981), migration of self-antigen-loaded DCs to the draining LN had not been experimentally verified. Here, we demonstrated that naive α MyHC-reactive TCR-M cells proliferated in the heart-draining mLN without inducing cardiac damage and that they partially adopted an iTreg phenotype. It has recently been shown that cDC1s and cDC2s can induce iTregs in mesenteric LNs, with redundancy observed in mice lacking either cDC1s or cDC2s (Esterházy et al., 2016). Accordingly, while observing a reduction in iTreg generation in mLNs of steady-state *Irf8^{fl/fl}.Cd11cCre* mice, the lack of cDC1s did not disrupt cardiac tolerance (unpublished data). We speculate that there is some redundancy among cardiac cDC subsets, which prevents autoimmunity in the absence of cDC1s.

Consistent with studies examining all DCs (Anzai et al., 2012; Zhang et al., 1993), we observed a significant yet transient increase in cardiac DC subsets post MI. RNA-seq analysis revealed that although heart cDC subsets retained their hallmark genes, the ischemic environment induced some changes compared with steady-state DCs. Analysis of DEGs identified a core MI signature, proposing that DCs from the infarcted heart had a more activated phenotype. Analysis of maturation markers confirmed this at the protein level. This is consistent with reports demonstrating that necrotic cardiomyocytes release danger signals, including Hsp70 (Maekawa et al., 2009), interleukin-1 α , and HMGB-1 (Zhang et al., 2015), which can promote DC activation

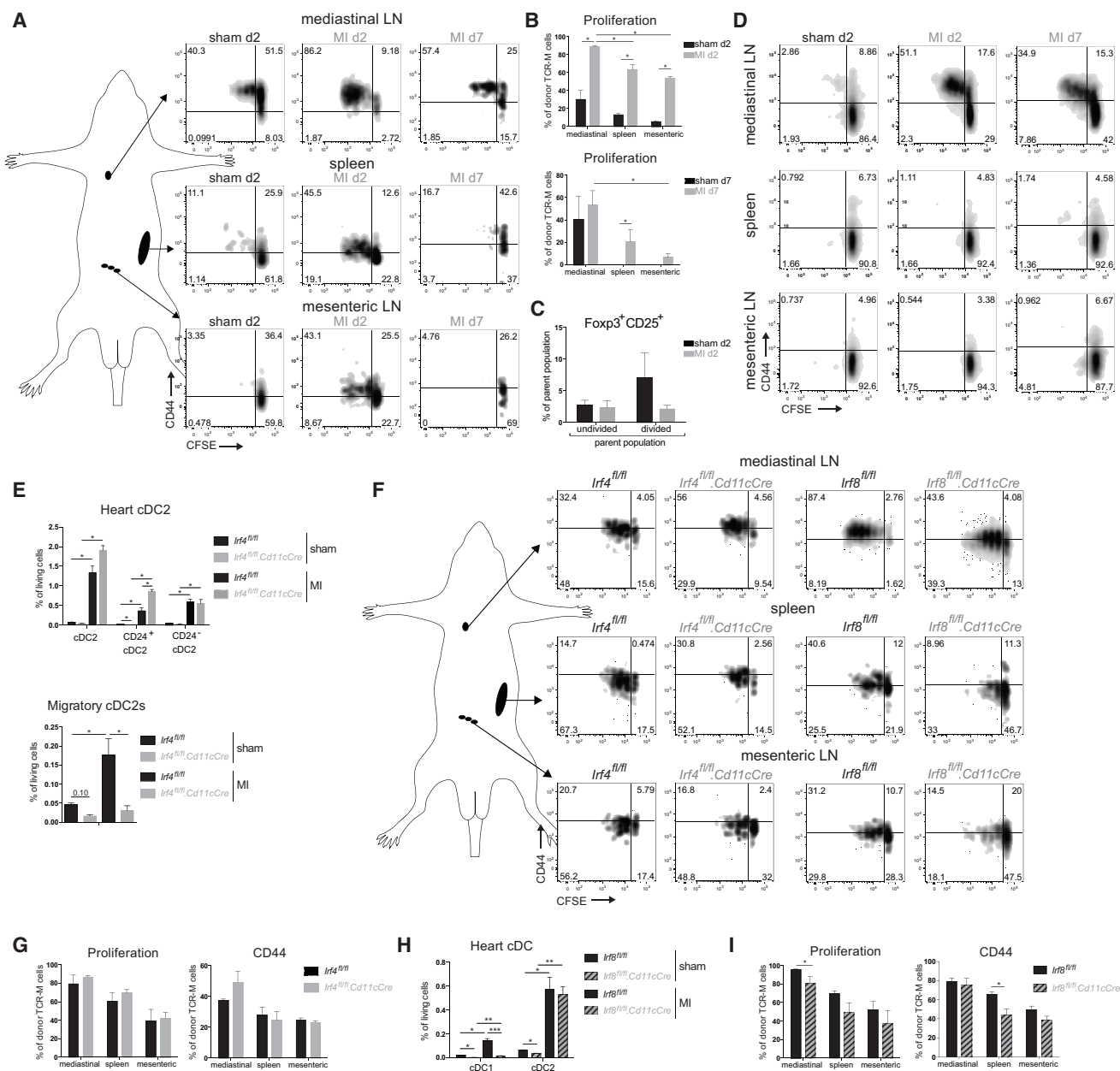


Figure 7. Myocardial Infarction Activates Autoreactive CD4⁺ T Cells In Vivo

(A) TCR-M cells were injected into sham or MI mice on day 2 or day 7 post-surgery. CFSE dilution and CD44 expression of donor TCR-M cells is shown.

(B) Proliferation of donor TCR-M cells in lymphoid organs from the experiment described in (A).

(C) Percentage of Foxp3/CD25 expression on undivided and divided donor TCR-M cells isolated from mLN in sham and MI mice at day 2 post-surgery.

(D) CFSE dilution and CD44 expression of naive TCR-M cells in ex vivo co-culture with bulk mediastinal LN, spleen, and mesenteric LN cells isolated from sham and MI mice on day 2 and day 7 post-surgery.

(E) Heart cDC2 and migratory cDC2 percentages in mLN of sham and MI *Irf4^{fl/fl}* and *Irf4^{fl/fl}.Cd11cCre* mice at day 7 post-surgery.

(F) *Irf4^{fl/fl}*, *Irf4^{fl/fl}.Cd11cCre*, *Irf8^{fl/fl}* and *Irf8^{fl/fl}.Cd11cCre* mice were injected with TCR-M cells at day 2 post MI. CFSE dilution and CD44 expression of donor TCR-M cells is shown.

(G) Proliferation and CD44 expression of donor TCR-M cells in LNs and spleen from *Irf4^{fl/fl}* and *Irf4^{fl/fl}.Cd11cCre* mice from the experiment described in (F).

(H) Heart cDC percentages of sham and MI *Irf8^{fl/fl}* and *Irf8^{fl/fl}.Cd11cCre* mice at day 7 post-surgery.

(I) Proliferation and CD44 expression of donor TCR-M cells in LNs and spleen from *Irf8^{fl/fl}* and *Irf8^{fl/fl}.Cd11cCre* mice from the experiment described in (F). All bar graphs in Figure 7 show data as mean ± SEM (*p ≤ 0.05; **p ≤ 0.01; ***p ≤ 0.001), and all data are representative of two independent experiments.

by inducing Toll-like/interleukin-1 receptor signaling. Cardiomyocyte necrosis also results in the release of cardiac self-antigens, such as myosin and troponin, which are constrained in the healthy heart (Larue et al., 1991). Thus, hypothetically, heart DCs become activated via TLR stimulation by danger signals after MI and get loaded with self-antigen, licensing DCs for the activation of self-antigen-specific autoreactive T cells. Indeed, we found that DCs from the infarcted heart and mLN presented cardiac self-antigen to autoreactive CD4⁺ T cells, which adopted a Th1/Th17 effector phenotype. This suggests that ischemic heart injury leads to cardiac autoimmunity by acting on the DC activation state. Post-infarct autoimmunity is commonly observed, with one-third of patients showing a proliferative response to cardiac myosin (Moraru et al., 2006). Furthermore, post-infarct autoimmunity contributes to persistent myocardial inflammation, leading to further damage with pathological consequences (Gotumukkala et al., 2012). Early after MI (day 2), TCR-M cells proliferated vigorously in heart-draining mLN and, interestingly, also in non-heart draining LNs, which could suggest systemic release of self-antigen post MI due to massive destruction of cardiomyocytes, which is captured by LN-resident DCs. However, we did not observe a significant proliferation of TCR-M cells when cocultured with bulk spleen or mesenteric LN cells, suggesting that either no systemic α MyHC release occurred or the quantity of self-antigen in the circulation was too low to activate TCR-M cells *ex vivo*. The proliferated TCR-M cells in distant LNs could possibly also represent recirculating cells that had divided in the heart-draining mLN after their first division.

Among DCs, cDC2s were the main subset activating autoreactive CD4⁺ T cells post MI and inducing IL-17a and IFN γ in TCR-M cells. Despite this, cDC2s may not be necessary because TCR-M cells also proliferated in the mLN of *Irf4^{fl/fl}.Cd11cCre* mice, which have a severe reduction in migratory cDC2s. Unfortunately, no perfect model exists, which results in a complete and specific cDC2 ablation because the TFs regulating cDC2 development are still largely unknown and might largely overlap with moDCs and MFs. Although cDC2s highly express IRF4, removal of IRF4 only affects migration of cDC2s (Bajaña et al., 2012). Although we have recently described *Zeb2* to be a major TF for cDC2 development, *Zeb2* loss only results in ablation of a proportion of cDC2s (Scott et al., 2016).

Overall, we demonstrate that DCs in the ischemic heart are activated and loaded with self-antigen, licensing DCs for efficient autoreactive T cell activation. In the future, it will be of great interest to examine the activation state and function of human DCs isolated from the infarcted heart. This could open the door for therapeutics preventing DC maturation and self-antigen presentation, which could limit the onset of pathological cardiac autoimmunity following MI.

EXPERIMENTAL PROCEDURES

Mice

Wild-type BALB/c mice were purchased from Harlan. α MyHC-TCR transgenic mice (TCR-M) on BALB/c background were provided by B. Ludewig and previously described (Nindi et al., 2012). *Flt3l^{-/-}* mice were on a C57/BL6 background. *Irf4^{fl/fl}.Cd11cCre* and *Irf8^{fl/fl}.Cd11cCre* were backcrossed onto the BALB/c background for at least two generations. Mice were used between 5

and 12 weeks of age. The animal ethics committee of Inflammation Research Center (VIB-Ghent University) (IRC) approved all experiments.

Infarct Model

MI was induced by coronary artery ligation in female 8- to 12-week-old mice. Mice were anesthetized with nembutal, moved in the supine position on a heating pad, and intubated. Respiration was started using positive pressure (1.5 L 90 strokes/min), and the left thorax was opened in between the third intercostal space. The pericardium was opened, and the LAD was ligated proximal to the main branching. Discoloration of the ventricle was obvious, indicating proper LAD ligation. Sham operation incorporated all actions, except LAD ligation.

Flow Cytometric Analysis and Sorting

Organs were freshly isolated, and heart ventricles were flushed with PBS. Organs were manually cut in 0.5- to 1-mm pieces using scissors. Samples were enzymatically digested with 20 μ g/mL liberase TM (Roche) and 10 U DNase (Roche) in RPMI for 45 min at 37°C. Osmotic lysis buffer was added for 3' to remove erythrocytes. Single-cell suspensions were incubated with a mix of fluorescently labeled monoclonal antibodies (Abs) for 30' at 4°C. To reduce non-specific binding, 2.4G2 Fc receptor Ab was added. An overview of Abs and clones is found in the [Supplemental Information](#). To identify live cells, fixable viability dye eFluor 506 (eBioscience) was added. For intranuclear staining of TFs, cells were fixed using a Foxp3 fixation/permeabilization kit (eBioscience). Data were acquired on an LSR Fortessa cytometer (BD Biosciences). For cell sorting, a FACSAria high-speed sorter (BD Biosciences) was used. Final analysis and graphical output were performed using FlowJo software (Tree Star) and GraphPad Prism.

RNA Sequencing

cDC1s, cDC2s, moDCs, and MFs were sorted by FACS from 100 pooled steady-state and 12 pooled infarcted hearts (7 days post-surgery) of female WT BALB/c mice, and four independent sorts were performed. A maximum of 25,000 cells were sorted directly into 500- μ L buffer (RLT Plus; QIAGEN), and 5- μ L β -mercaptoethanol and RNA was isolated by using a micro-RNA isolation kit (QIAGEN). Because RNA amounts were low, RNA was amplified using SmarTER amplification (Clontech). RNA sequencing was executed at the Nucleomics facility (VIB) using the NextSeq sequencer (Illumina). RNA-seq was analyzed using Trimmomatic. All details are described in the [Supplemental Information](#).

Adoptive Transfer of TCR-M Cells

Spleens were collected from TCR-M mice and disrupted on a 70- μ m cell strainer. Naive TCR-M splenocytes were MACS purified using the CD4⁺CD62L⁺ T Cell isolation kit (Miltenyi). TCR-M cells were labeled with CFSE (Invitrogen). 1×10^6 naive TCR-M T cells were injected intravenously in the lateral tail vein of sham-operated and infarcted mice at day 2 and day 7 after surgery. 3 days after TCR-M adoptive transfer, mice were sacrificed, lymphoid organs were isolated, and cell suspensions were prepared as described for the spleen. CFSE dilution and T cell activation were evaluated by flow cytometry.

Ex Vivo Bulk Lymph Node Co-cultures

Lymph nodes were collected from mice at day 2 or day 7 post surgery. Single-cell suspensions were prepared as described above. 2.5×10^5 bulk LN cells were added to 5×10^4 MACS purified naive CD4⁺CD62L^{hi} TCR-M cells that were CFSE labeled. CFSE dilution and T cell activation were evaluated by flow cytometry after 3 days of incubation at 37°C, 5% CO₂, and 20% O₂.

Ex vivo Co-cultures of Sorted DC Subsets and TCR-M Cells

TCR-M cells were purified from the spleen using the CD4⁺ T Cell isolation kit (Miltenyi) and labeled with CFSE. 5×10^4 TCR-M cells were co-cultured with 1×10^4 FACS-sorted cDC1s, cDC2s, and moDCs from the mediastinal, mesenteric LN, or heart of sham and MI mice (day 7). CFSE dilution and T cell activation were evaluated by flow cytometry after 4 days of incubation at 37°C, 5% CO₂, and 20% O₂. To check Th skewing of TCR-M cells, IL-17A and IFN γ ELISA (eBioscience, Ready-Set-Go kit) was performed on the co-culture cell supernatants.

Statistical Analysis

For all experiments, the difference between groups was calculated using the Mann-Whitney *U* test for unpaired data (GraphPad Prism) and was considered significant when $p < 0.05$.

ACCESSION NUMBERS

The accession number for all RNA-sequencing data reported in this paper is GEO: GSE94949.

SUPPLEMENTAL INFORMATION

Supplemental Information includes Supplemental Experimental Procedures, one figure, and eight tables and can be found with this article online at <http://dx.doi.org/10.1016/j.celrep.2017.02.079>.

AUTHOR CONTRIBUTIONS

Conceptualization, B.N.L. and P.C.; Methodology, K.V.d.B., D.S., C.L.S., P.C., and M.G.; Formal Analysis; L.M.; Investigation, A.B., J.V.M., M.V., and S.D.P.; Resources, V.N. and B.L.; Writing – Original Draft, K.V.d.B.; Writing – Review & Editing, C.L.S. and B.N.L.; Funding Acquisition, B.N.L. and T.G.; Supervision; B.N.L., T.G., and C.L.S. B.N.L. and P.C. shared supervision over the work.

ACKNOWLEDGMENTS

K.V.d.B. was supported by an AAP fellowship of Ghent University. C.L.S. is supported by a Marie Curie Intra-European Fellowship (IEF; H2020-MSCA-IF-2014 660448). B.N.L. is supported by several FWO grants (Fonds Wetenschappelijk Onderzoek, Vlaanderen) and is the recipient of an ERC consolidator grant (41D04510W).

Received: October 3, 2016

Revised: January 18, 2017

Accepted: February 27, 2017

Published: March 21, 2017

REFERENCES

- Anzai, A., Anzai, T., Nagai, S., Maekawa, Y., Naito, K., Kaneko, H., Sugano, Y., Takahashi, T., Abe, H., Mochizuki, S., et al. (2012). Regulatory role of dendritic cells in postinfarction healing and left ventricular remodeling. *Circulation* *125*, 1234–1245.
- Ardouin, L., Luche, H., Chelbi, R., Carpentier, S., Shawket, A., Montanana Sanchez, F., Santa Maria, C., Grenot, P., Alexandre, Y., Grégoire, C., et al. (2016). Broad and largely concordant molecular changes characterize tolerogenic and immunogenic dendritic cell maturation in thymus and periphery. *Immunity* *45*, 305–318.
- Bajaña, S., Roach, K., Turner, S., Paul, J., and Kovats, S. (2012). IRF4 promotes cutaneous dendritic cell migration to lymph nodes during homeostasis and inflammation. *J. Immunol.* *189*, 3368–3377.
- Bajaña, S., Turner, S., Paul, J., Ainsua-Enrich, E., and Kovats, S. (2016). IRF4 and IRF8 act in CD11c+ cells to regulate terminal differentiation of lung tissue dendritic cells. *J. Immunol.* *196*, 1666–1677.
- Caton, M.L., Smith-Raska, M.R., and Reizis, B. (2007). Notch-RBP-J signaling controls the homeostasis of CD8- dendritic cells in the spleen. *J. Exp. Med.* *204*, 1653–1664.
- Darrasse-Jéze, G., Deroubaix, S., Mouquet, H., Victoria, G.D., Eisenreich, T., Yao, K.H., Masilamani, R.F., Dustin, M.L., Rudensky, A., Liu, K., and Nussenzweig, M.C. (2009). Feedback control of regulatory T cell homeostasis by dendritic cells in vivo. *J. Exp. Med.* *206*, 1853–1862.
- Davis, M.M. (2015). Not-so-negative selection. *Immunity* *43*, 833–835.
- Epelman, S., Lavine, K.J., Beaudin, A.E., Sojka, D.K., Carrero, J.A., Calderon, B., Brijia, T., Gautier, E.L., Ivanov, S., Satpathy, A.T., et al. (2014). Embryonic and adult-derived resident cardiac macrophages are maintained through distinct mechanisms at steady state and during inflammation. *Immunity* *40*, 91–104.
- Eriksson, U., Ricci, R., Hunziker, L., Kurrer, M.O., Oudit, G.Y., Watts, T.H., Sonderegger, I., Bachmaier, K., Kopf, M., and Penninger, J.M. (2003). Dendritic cell-induced autoimmune heart failure requires cooperation between adaptive and innate immunity. *Nat. Med.* *9*, 1484–1490.
- Esterházy, D., Loschko, J., London, M., Jove, V., Oliveira, T.Y., and Mucida, D. (2016). Classical dendritic cells are required for dietary antigen-mediated induction of peripheral T(reg) cells and tolerance. *Nat. Immunol.* *17*, 545–555.
- Gallucci, S., Lolkema, M., and Matzinger, P. (1999). Natural adjuvants: endogenous activators of dendritic cells. *Nat. Med.* *5*, 1249–1255.
- Gangaplara, A., Massilamany, C., Brown, D.M., Delhon, G., Pattnaik, A.K., Chapman, N., Rose, N., Steffen, D., and Reddy, J. (2012). Coxsackievirus B3 infection leads to the generation of cardiac myosin heavy chain- α -reactive CD4 T cells in A/J mice. *Clin. Immunol.* *144*, 237–249.
- Ganguly, D., Haak, S., Sisirak, V., and Reizis, B. (2013). The role of dendritic cells in autoimmunity. *Nat. Rev. Immunol.* *13*, 566–577.
- Gawden-Bone, C., Zhou, Z., King, E., Prescott, A., Watts, C., and Lucocq, J. (2010). Dendritic cell podosomes are protrusive and invade the extracellular matrix using metalloproteinase MMP-14. *J. Cell Sci.* *123*, 1427–1437.
- Gottumukkala, R.V., Lv, H., Cornivelli, L., Wagers, A.J., Kwong, R.Y., Bronson, R., Stewart, G.C., Schulze, P.C., Chutkow, W., Wolpert, H.A., et al. (2012). Myocardial infarction triggers chronic cardiac autoimmunity in type 1 diabetes. *Sci. Transl. Med.* *4*, 138ra80.
- Guilliams, M., Ginhoux, F., Jakubzick, C., Naik, S.H., Onai, N., Schraml, B.U., Segura, E., Tussiwand, R., and Yona, S. (2014). Dendritic cells, monocytes and macrophages: a unified nomenclature based on ontogeny. *Nat. Rev. Immunol.* *14*, 571–578.
- Guilliams, M., Dutertre, C.A., Scott, C.L., McGovern, N., Sichien, D., Chakarova, S., Van Gassen, S., Chen, J., Poidinger, M., De Prijck, S., et al. (2016). Unsupervised high-dimensional analysis aligns dendritic cells across tissues and species. *Immunity* *45*, 669–684.
- Gurka, S., Hartung, E., Becker, M., and Kroczeck, R.A. (2015). Mouse conventional dendritic cells can be universally classified based on the mutually exclusive expression of XCR1 and SIRP α . *Front. Immunol.* *6*, 35.
- Hart, D.N., and Fabre, J.W. (1981). Demonstration and characterization of Ia-positive dendritic cells in the interstitial connective tissues of rat heart and other tissues, but not brain. *J. Exp. Med.* *154*, 347–361.
- Heinz, L.X., Baumann, C.L., Köberlin, M.S., Snijder, B., Gawish, R., Shui, G., Sharif, O., Aspalter, I.M., Müller, A.C., Kandasamy, R.K., et al. (2015). The lipid-modifying enzyme SMPDL3B negatively regulates innate immunity. *Cell Rep.* *11*, 1919–1928.
- Holst, K., Guseva, D., Schindler, S., Sixt, M., Braun, A., Chopra, H., Pabst, O., and Ponimaskin, E. (2015). The serotonin receptor 5-HT $_7$ R regulates the morphology and migratory properties of dendritic cells. *J. Cell Sci.* *128*, 2866–2880.
- Kool, M., van Loo, G., Waelput, W., De Prijck, S., Muskens, F., Sze, M., van Praet, J., Branco-Madeira, F., Janssens, S., Reizis, B., et al. (2011). The ubiquitin-editing protein A20 prevents dendritic cell activation, recognition of apoptotic cells, and systemic autoimmunity. *Immunity* *35*, 82–96.
- Larue, C., Calzolari, C., Léger, J., Léger, J., and Pau, B. (1991). Immunoradiometric assay of myosin heavy chain fragments in plasma for investigation of myocardial infarction. *Clin. Chem.* *37*, 78–82.
- Latet, S.C., Hoymans, V.Y., Van Herck, P.L., and Vrints, C.J. (2015). The cellular immune system in the post-myocardial infarction repair process. *Int. J. Cardiol.* *179*, 240–247.
- Lipes, M.A., and Galderisi, A. (2015). Cardiac autoimmunity as a novel biomarker, mediator, and therapeutic target of heart disease in type 1 diabetes. *Curr. Diab. Rep.* *15*, 30.
- Lv, H., and Lipes, M.A. (2012). Role of impaired central tolerance to α -myosin in inflammatory heart disease. *Trends Cardiovasc. Med.* *22*, 113–117.
- Lv, H., Havari, E., Pinto, S., Gottumukkala, R.V., Cornivelli, L., Raddassi, K., Matsui, T., Rosenzweig, A., Bronson, R.T., Smith, R., et al. (2011). Impaired

- thymic tolerance to α -myosin directs autoimmunity to the heart in mice and humans. *J. Clin. Invest.* **121**, 1561–1573.
- Maekawa, Y., Mizue, N., Chan, A., Shi, Y., Liu, Y., Dawood, S., Chen, M., Dawood, F., de Couto, G., Li, G.H., et al. (2009). Survival and cardiac remodeling after myocardial infarction are critically dependent on the host innate immune interleukin-1 receptor-associated kinase-4 signaling: a regulator of bone marrow-derived dendritic cells. *Circulation* **120**, 1401–1414.
- Magister, S., Obermajer, N., Mirković, B., Svaiger, U., Renko, M., Softić, A., Romih, R., Colbert, J.D., Watts, C., and Kos, J. (2012). Regulation of cathepsins S and L by cystatin F during maturation of dendritic cells. *Eur. J. Cell Biol.* **91**, 391–401.
- Mildner, A., and Jung, S. (2014). Development and function of dendritic cell subsets. *Immunity* **40**, 642–656.
- Miller, J.C., Brown, B.D., Shay, T., Gautier, E.L., Jojic, V., Cohain, A., Pandey, G., Leboeuf, M., Elpek, K.G., Helft, J., et al.; Immunological Genome Consortium (2012). Deciphering the transcriptional network of the dendritic cell lineage. *Nat. Immunol.* **13**, 888–899.
- Molawi, K., Wolf, Y., Kandalla, P.K., Favret, J., Hagemeyer, N., Frenzel, K., Pinto, A.R., Klapproth, K., Henri, S., Malissen, B., et al. (2014). Progressive replacement of embryo-derived cardiac macrophages with age. *J. Exp. Med.* **211**, 2151–2158.
- Moraru, M., Roth, A., Keren, G., and George, J. (2006). Cellular autoimmunity to cardiac myosin in patients with a recent myocardial infarction. *Int. J. Cardiol.* **107**, 61–66.
- Nindl, V., Maier, R., Ratering, D., De Giulii, R., Züst, R., Thiel, V., Scandella, E., Di Padova, F., Kopf, M., Rudin, M., et al. (2012). Cooperation of Th1 and Th17 cells determines transition from autoimmune myocarditis to dilated cardiomyopathy. *Eur. J. Immunol.* **42**, 2311–2321.
- Ohl, L., Mohaupt, M., Czeloth, N., Hintzen, G., Kiafard, Z., Zwirner, J., Blankenstein, T., Henning, G., and Förster, R. (2004). CCR7 governs skin dendritic cell migration under inflammatory and steady-state conditions. *Immunity* **21**, 279–288.
- Ohnmacht, C., Pullner, A., King, S.B.S., Drexler, I., Meier, S., Bocker, T., and Voehringer, D. (2009). Constitutive ablation of dendritic cells breaks self-tolerance of CD4 T cells and results in spontaneous fatal autoimmunity. *J. Exp. Med.* **206**, 549–559.
- Persson, E.K., Uronen-Hansson, H., Semmrich, M., Rivollier, A., Hägerbrand, K., Marsal, J., Gudjonsson, S., Håkansson, U., Reizis, B., Kotarsky, K., et al. (2013). IRF4 transcription-factor-dependent CD103(+)CD11b(+) dendritic cells drive mucosal T helper 17 cell differentiation. *Immunity* **38**, 958–969.
- Scaffidi, P., Misteli, T., and Bianchi, M.E. (2002). Release of chromatin protein HMGB1 by necrotic cells triggers inflammation. *Nature* **418**, 191–195.
- Scott, C.L., Bain, C.C., Wright, P.B., Sichien, D., Kotarsky, K., Persson, E.K., Luda, K., Williams, M., Lambrecht, B.N., Agace, W.W., et al. (2015). CCR2(+)CD103(-) intestinal dendritic cells develop from DC-committed precursors and induce interleukin-17 production by T cells. *Mucosal Immunol.* **8**, 327–339.
- Scott, C.L., Soen, B., Martens, L., Skrypek, N., Saelens, W., Taminau, J., Blancke, G., Van Isterdael, G., Huylebroeck, D., Haigh, J., et al. (2016). The transcription factor Zeb2 regulates development of conventional and plasmacytoid DCs by repressing Id2. *J. Exp. Med.* **213**, 897–911.
- Sichien, D., Scott, C.L., Martens, L., Vanderkerken, M., Van Gassen, S., Plantinga, M., Joeris, T., De Prijck, S., Vanhoutte, L., Vanheerswynghels, M., et al. (2016). IRF8 transcription factor controls survival and function of terminally differentiated conventional and plasmacytoid dendritic cells, respectively. *Immunity* **45**, 626–640.
- Sichien, D., Lambrecht, B.N., Williams, M., and Scott, C.L. (2017). Development of conventional dendritic cells: from common bone marrow progenitors to multiple subsets in peripheral tissues. *Mucosal Immunol.* Published online February 15, 2017. <http://dx.doi.org/10.1038/mi.2017.8>.
- Steinman, R.M., Hawiger, D., and Nussenzweig, M.C. (2003). Tolerogenic dendritic cells. *Annu. Rev. Immunol.* **21**, 685–711.
- Stranges, P.B., Watson, J., Cooper, C.J., Choisy-Rossi, C.M., Stonebraker, A.C., Beighton, R.A., Hartig, H., Sundberg, J.P., Servick, S., Kaufmann, G., et al. (2007). Elimination of antigen-presenting cells and autoreactive T cells by Fas contributes to prevention of autoimmunity. *Immunity* **26**, 629–641.
- Tamoutounour, S., Williams, M., Montanana Sanchis, F., Liu, H., Terhorst, D., Malosse, C., Pollet, E., Ardouin, L., Lucche, H., Sanchez, C., et al. (2013). Origins and functional specialization of macrophages and of conventional and monocyte-derived dendritic cells in mouse skin. *Immunity* **39**, 925–938.
- Tian, W., Nunez, R., Cheng, S., Ding, Y., Tumang, J., Lyddane, C., Roman, C., and Liou, H.C. (2005). C-type lectin OCILRP2/C1r-g and its ligand NKRPF costimulate T cell proliferation and IL-2 production. *Cell. Immunol.* **234**, 39–53.
- Torchinsky, M.B., Garaude, J., Martin, A.P., and Blander, J.M. (2009). Innate immune recognition of infected apoptotic cells directs T(H)17 cell differentiation. *Nature* **458**, 78–82.
- Waskow, C., Liu, K., Darrasse-Jèze, G., Guermontprez, P., Ginhoux, F., Merad, M., Shengelia, T., Yao, K., and Nussenzweig, M. (2008). The receptor tyrosine kinase Flt3 is required for dendritic cell development in peripheral lymphoid tissues. *Nat. Immunol.* **9**, 676–683.
- Wu, X., Briseño, C.G., Durai, V., Albring, J.C., Haldar, M., Bagadia, P., Kim, K.W., Randolph, G.J., Murphy, T.L., and Murphy, K.M. (2016). MafB lineage tracing to distinguish macrophages from other immune lineages reveals dual identity of Langerhans cells. *J. Exp. Med.* **213**, 2553–2565.
- Zhang, J., Yu, Z.X., Fujita, S., Yamaguchi, M.L., and Ferrans, V.J. (1993). Interstitial dendritic cells of the rat heart. Quantitative and ultrastructural changes in experimental myocardial infarction. *Circulation* **87**, 909–920.
- Zhang, W., Lavine, K.J., Epelman, S., Evans, S.A., Weinheimer, C.J., Barger, P.M., and Mann, D.L. (2015). Necrotic myocardial cells release damage-associated molecular patterns that provoke fibroblast activation in vitro and trigger myocardial inflammation and fibrosis in vivo. *J. Am. Heart Assoc.* **4**, e001993.
- Zigmond, E., Samia-Grinberg, S., Pasmanik-Chor, M., Brazowski, E., Shibolet, O., Halpern, Z., and Varol, C. (2014). Infiltrating monocyte-derived macrophages and resident kupffer cells display different ontogeny and functions in acute liver injury. *J. Immunol.* **193**, 344–353.